catalysts

MDPI

Article

From Enzyme to Preparative Cascade Reactions with Immobilized Enzymes: Tuning Fe(II)/α-Ketoglutarate-Dependent Lysine Hydroxylases for Application in Biotransformations

Selina Seide, Lilia Arnold, Solange Wetzels, Mariela Bregu, Jochem Gätgens and Martina Pohl *

IBG-1: Biotechnology, Forschungszentrum Jülich GmbH, 52425 Jülich, Germany; s.seide@fz-juelich.de (S.S.); li.arnold@fz-juelich.de (L.A.); s.wetzels@fz-juelich.de (S.W.); m.bregu@fz-juelich.de (M.B.); j.gaetgens@fz-juelich.de (J.G.)
* Correspondence: ma.pohl@fz-juelich.de; Tel.: +49-246-161-4388

Abstract: Fe(II)/α-ketoglutarate-dependent dioxygenases (KDOs) catalyze a broad range of selective C–H oxidation reactions. However, the difficult production of KDOs in recombinant *E. coli* strains and their instability in purified form have so far limited their application in preparative biotransformations. Here, we investigated the immobilization of three KDOs (*Ca*KDO, *Cp*KDO, *Fj*KDO) that catalyze the stereoselective hydroxylation of the L-lysine side chain using two one-step immobilization techniques (HaloTag®, EziG™). The HaloTag®-based immobilisates reached the best results with respect to residual activity and stability. In preparative lab-scale experiments, we achieved product titers of 16 g L^{-1} (3*S*)-hydroxy-L-lysine (*Ca*KDO) and (4*R*)-hydroxy-L-lysine (*Fj*KDO), respectively, starting from 100 mM L-lysine. Using a HaloTag®-immobilized lysine decarboxylase from *Selenomonas ruminantium* (*Sr*LDC), the (3*S*)-hydroxy-L-lysine from the *Ca*KDO-catalyzed reaction was successfully converted to (2*S*)-hydroxy-cadaverine without intermediate product purification, yielding a product titer of 11.6 g L^{-1} in a 15 mL consecutive batch reaction. We propose that covalent in situ immobilization is an appropriate tool to access the preparative potential of many other KDOs.

Keywords: 2-oxoglutarate-dependent oxygenases; hydroxylation; amino acid modification; 1,5-diamino pentane; 1,5-diaminopentane-(2*S*)-ol; L-ornithine; 1,4-diaminobutan; OPA derivatization; repetitive batch; cascade reaction

Citation: Seide, S.; Arnold, L.; Wetzels, S.; Bregu, M.; Gätgens, J.; Pohl, M. From Enzyme to Preparative Cascade Reactions with Immobilized Enzymes: Tuning Fe(II)/α-Ketoglutarate-Dependent Lysine Hydroxylases for Application in Biotransformations. *Catalysts* **2022**, *12*, 354. https://doi.org/10.3390/catal12040354

Academic Editor: Evangelos Topakas

Received: 25 February 2022
Accepted: 17 March 2022
Published: 22 March 2022

1. Introduction

C–H functionalization is a chemically challenging reaction because carbon hydrogen bonds are relatively inert, making chemo-, regio-, and stereo-selectivity hard to control with conventional chemical catalysts [1]. The most commonly used enzyme class for such reactions up to now is P450 monooxygenases. However, the application of these enzymes on a preparative scale is often limited due to issues with inefficient electron transfer, uncoupling reactions, low activity and stability, and the requirement of expensive redox cofactors [2,3]. Another promising enzyme class for C–H functionalization are non-heme Fe(II)/α-ketoglutarate-dependent dioxygenases (KDOs, EC 1.14.11.), which make up a large superfamily of enzymes utilizing Fe(II) as a cofactor. KDOs catalyze the oxidative decarboxylation of their cosubstrate α-ketoglutarate (α-KG) towards succinate and CO_2. The enzymatic reaction activates O_2, which then can be used in a set of different oxidation reactions including hydroxylation, halogenation, ring closure, desaturation, epimerization, ring expansion, and epoxidation [4–8]. A great advantage of KDOs is that they are self-sufficient, as they do not need specific reductases or expensive biological redox cofactors. Many KDOs are associated with natural product biosynthesis pathways in bacteria, fungi, plants, and vertebrates, where the most studied pathways include the biosynthesis of

antibiotics such as penicillin, cephalosporin, cephamycin, and clavam [4,8]. The number of different chemically challenging reactions that this enzyme class is able to catalyze makes them an interesting target for biocatalytic applications [7].

The most common industrial application of KDOs is the stereoselective hydroxylation of amino acids. The resulting products serve as precursors for the chemical and pharmaceutical industry, as was recently extensively reviewed by Peters and Buller [7].

Chiral hydroxy-L-lysines are used as chiral auxiliaries [7], as precursors for active pharmaceutical ingredients, such as the HIV protease inhibitor palinavir [9,10], for potential novel anticancer drugs such as tambromycin [11], the protein kinase c inhibitor (-) balanol [12], and the proteasome inhibitors cepafungin I or glidobactin A [13,14]. Lysine, ornithine and its hydroxylated derivatives are also precursors for polyamides, as their decarboxylation yields the respective terminal diamines, such as putrescine, cadaverine, and hydroxylated derivatives thereof, which can be used for the production of novel (fully) bio-based polyamides. The resulting bio-polyamide nylon 5X materials have excellent properties, even superior to petroleum-based nylon 6.6 [15–17]. Additional hydroxyl groups can undergo various reactions, such as esterification, or they can act as initiation sites for ring opening polymerizations of cyclic esters [18–20]. Thus, hydroxylated diamines could provide access to functionalized polymers [21].

Meanwhile, several L-lysine hydroxylases for the stereoselective hydroxylation of the L-lysine side chain in either the 3- or 4-position are known. KDOs from *Catenulispora acidiphila* (*Ca*KDO, KDO1: 3-hydroxylation), *Chitinophaga pinensis* (*Cp*KDO, KDO2: 4-hydroxylation), and *Flavobacterium johnsoniae* (*Fj*KDO, KDO3: 4-hydroxylation) have recently been discovered by Baud et al. [22,23] (Figure 1). At the same time, Hara et al. independently discovered K4H-2 and K4H-1, which correspond to *Cp*KDO and *Fj*KDO, respectively [24]. The crystal structures of *Ca*KDO and another KDO from *Flavobacterium species* (*Fs*KDO, KDO5) were solved, demonstrating the typical double-stranded β-helix core structure of the α-KG-dependent oxygenase structural superfamily [25,26]. In the crystal structure, both enzymes show two dimers per asymmetric unit, whereas their quaternary structure in solution is different: dimeric in the case of *Ca*KDO and tetrameric for *Fs*KDO [25].

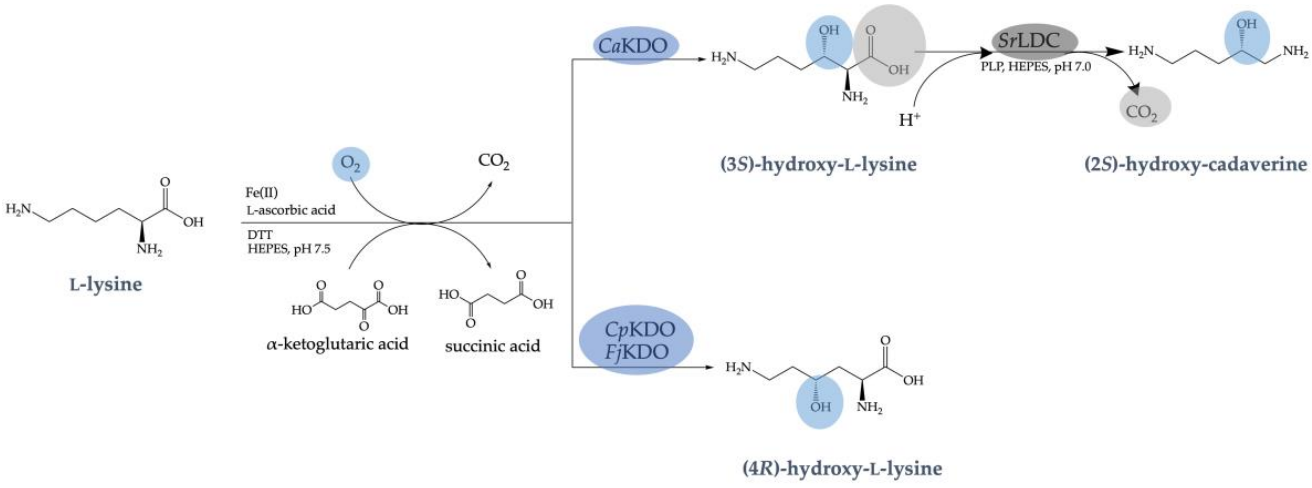

Figure 1. Reaction scheme of the stereoselective hydroxylation of the L-lysine side chain in the 4-position catalyzed by KDO from *Chitinophaga pinensis* (*Cp*KDO) and KDO from *Flavobacterium johnsoniae* (*Fj*KDO) or in the 3-position catalyzed by KDO from *Catenulispora acidiphila* (*Ca*KDO) followed by decarboxylation to (2S)-hydroxy cadaverine catalyzed by *Sr*LDC from *Selenomonas ruminantium*.

Three major problems tend to occur when working with KDOs in general:

(1) The enzyme yield from recombinant *E. coli* hosts is often low with a large fraction of insoluble non-active inclusion bodies, which can be partly prevented by coexpression of chaperones [11,13,27–29];
(2) Purification and storage of these enzymes is challenging, due to the requirement of Fe(II) as a cofactor, which must be prevented from oxidation and dissociation from the active site [25,29];
(3) Precipitation occurs under oxidative conditions due to the instability of the enzyme [28,29].

Therefore, most applications of KDOs in biotransformation employ whole recombinant cells or respective cell-free extracts [11,13,14,24,27]. Since some KDOs, such as *Ca*KDO, *Cp*KDO, and *Fj*KDO, show very low specific activities [23], high concentrations of whole cells [24] or cell-free extracts [11] are required. In both cases, side reactions may occur due to the (potentially higher) activity of other enzymes. Mass transfer, oxygen transfer, and product separation are also often hampered by the high concentration of cellular components. In comparison, working with isolated enzymes allows a much more flexible process optimization [28,30]. On the other hand, enzyme purification is expensive; soluble enzymes often have low stability; they cannot be recycled and might complicate reaction engineering and product purification, as in the case of whole cells and cell-free extracts. Furthermore, the enzyme is usually the biggest cost factor in enzyme-catalyzed syntheses [31]. Thus, efficient immobilization techniques are crucial to increase process economy specifically for complex enzymes such as KDOs that are difficult to produce and show only low activity [23]. Thus, we tested two different one-step immobilization techniques to concentrate the biocatalyst directly from crude-cell extracts, increase its stability, and enable recycling.

There is hardly any application of immobilized KDOs in the literature, probably because many immobilization techniques require purified enzymes beforehand. During the course of this study, the Kourist group published the application of immobilized N-succinyl-L-amino acid dioxygenase SadA on EziG™ Amber for the production of N-succinyl-β-hydroxy-L-valine on a preparative lab scale [28]. EziG™ consists of a specific controlled pore glass (CPG), coated with an organic polymer layer, and was recently developed as a one-step immobilization from cell-free extracts for proteins with a poly-histidine tag [32]. Instead of nickel or cobalt ions, iron is chelated on the surface of the respectively modified carriers. EziG™ beads are available with three surface modifications with different hydrophobicity: Amber, Coral, and Opal. The advantage of this non-covalent immobilization technique is the recycling of the carrier by removing inactive enzyme with imidazole. On the other hand, a clear disadvantage is possible enzyme leakage. Here, covalent immobilization using HaloTag® represents a good alternative. HaloTag® is a mutated dehalogenase, which recognizes terminal chloroalkane residues on any respectively modified carrier material and instantly forms a covalent ester bond between the carrier, e.g., commercially available HaloLink™ resin, and an aspartate residue in the active site of HaloTag® [33,34]. The advantage of this covalent immobilization technique is the prevention of enzyme leakage and the high residual activity of 35–65% relative to the soluble enzyme [34–36]. In addition, HaloTag® can enhance protein solubility, which is specifically advantageous to prevent the inclusion body formation of respective fusion proteins [37].

In this study, three different KDOs, which catalyze the stereoselective hydroxylation of the L-lysine side chain in the 3-position (*Ca*KDO from *Catenulispora acidiphila)* and the 4-position (*Cp*KDO from *Chitinophaga pinensis* or *Fj*KDO from *Flavobacterium johnsoniae)* [22,23], were investigated for their potential application in a preparative lab scale. First, KDO production and purification were optimized in order to increase the soluble protein production and enzyme stability during purification. Then, we tested two one-step immobilization techniques (HaloTag®, EziG™), followed by application of all three KDO-HaloTag® variants immobilized on HaloLink™ resin in repetitive batch experiments.

HaloTag®-immobilized *Ca*KDO and *Fj*KDO were then selected for preparative-scale biotransformations.

Finally, *Ca*KDO and a lysine decarboxylase from *Selenomonas ruminantium* (*Sr*LDC) [23], both immobilized on HaloLink™ resin, were combined in a cascade reaction for the production of (2*S*)-hydroxy cadaverine (Figure 1).

2. Results

2.1. KDO Production and Purification

In the present study, a previously described protocol for *Ca*KDO production using coexpressed chaperones (GroEL/GroES) [11] was successfully applied to enhance the soluble production of *Ca*KDO, *Cp*KDO, and especially, *Fj*KDO, as well as for their HaloTag® fusions (Supplementary Materials, Figure S1). Without coexpression of chaperones, these enzymes were barely active and rapidly precipitated already from the cell-free extracts (data not shown). As can be seen by SDS-PAGE analysis, chaperones are still present even after purification and immobilization (Supplementary Materials, Figures S1 and S2) due to obviously strong binding to the target enzyme, which was described for several proteins before [38].

Initial tests demonstrated that freeze-drying is the best option to maintain the activity of KDOs after immobilized metal affinity chromatography (IMAC), which prevents using HEPES buffer or the addition of 10vol% glycerin, which both stabilize the enzymes in solution for a short time (data not shown). As earlier reported [29], we also observed the loss of activity after elution from IMAC when we tried to purify *Cp*KDO in TRIS buffer (Supplementary Materials, Figure S6B). Since *Ca*KDO and *Fs*KDO showed a higher degree of ordered structure in structural investigations upon binding of Fe(II) and α-KG [25], we presumed a positive effect on the enzyme stability upon addition of these cofactors and optimized the IMAC purification protocol, respectively. We used a combination of sodium phosphate buffer with low concentrations of the cosubstrate α-KG, as well as L-ascorbic acid and dithiothreitol (DTT) as reducing agents. Precipitation and inactivation of all three KDOs was successfully prevented by the addition of the Fe(II) cofactor immediately after IMAC, and the desalting step took place in the presence of α-KG, Fe(II) and the reducing agents, followed by lyophilization of the enzyme from the same mixture (Supplementary Materials, Section S2.1.2).

While we were able to improve the soluble KDO production and purification, purification of these enzymes is laborious and costly, and the enzyme yield is low. Furthermore, all components applied during the desalting step contaminate the lyophilisate, decreasing the protein content to 10–35%. This and the low enzyme yield consequently lead to problems when utilizing the lyophilisate for reactions. Furthermore, precipitation due to the instability of purified *Ca*KDO during biotransformation remains an issue (Supplementary Materials, Figure S7).

2.2. Immobilization and Reaction Optimization with KDOs

We tested the immobilization of KDOs as a suitable reaction engineering approach to increase enzyme stability and avoid enzyme purification, simultaneously, and compared two simple one-step immobilization techniques that allow immobilization directly from the cell-free extract: HaloTag® and EziG™.

In order to investigate the binding capacities of the different carriers, we quantified the enzyme concentration on the beads using the BCA assay (Supplementary Materials, Section S3.1.1) and confirmed the enzyme immobilization qualitatively by SDS PAGE (Supplementary Materials, Figure S8). Loading of the HaloLink™ resin reached 4.8 mg mL^{-1}_{resin} for *Ca*KDO-HaloTag®, 7.0 mg mL^{-1}_{resin} *Cp*KDO-HaloTag®, and 5.6 mg mL^{-1}_{resin} *Fj*KDO-HaloTag®, which is in line with the manufacturer's information of 7 mg of enzyme per mL HaloLink™ resin (Supplementary Materials, Table S3). For the three different EziG™ beads, only 0.11–0.16 mg *Ca*KDO, 0.03–0.05 mg *Cp*KDO, and 0.03–0.06 mg *Fj*KDO were bound per mg of beads (Supplementary Materials, Table S3), representing 3–16% *w/w* of the binding

capacity. This is lower or in the lower range of the binding capacities specified in the manufacturer's information (15–60% *w*/*w*) [32,39].

Both immobilization techniques were compared by measuring the specific activities of the immobilisates relative to the free purified enzymes with His-Tag (Figure 2A). Immobilization of *Ca*KDO via HaloTag®, EziG™ Amber, and Opal increased the specific activities, with the HaloTag® immobilisate showing the highest residual activity (280 ± 39%) compared to the free enzyme without HaloTag®. The EziG™ Coral immobilisate showed similar specific activity compared to the free enzyme (95 ± 0.9%). For *Cp*KDO, all immobilized variants were less active compared to the free enzyme. The highest residual activity was measured with the HaloTag® immobilisate (70 ± 1.5%). Likewise, all immobilized *Fj*KDO preparations were less active than the free variant, with the highest residual activity (62 ± 7.6%) for the EziG™ Opal variant. Here, the HaloTag® immobilization resulted in only moderate residual activities of about 43 ± 0.3% (Figure 2A). These results demonstrate again the different performance of immobilization strategies even with highly similar enzymes.

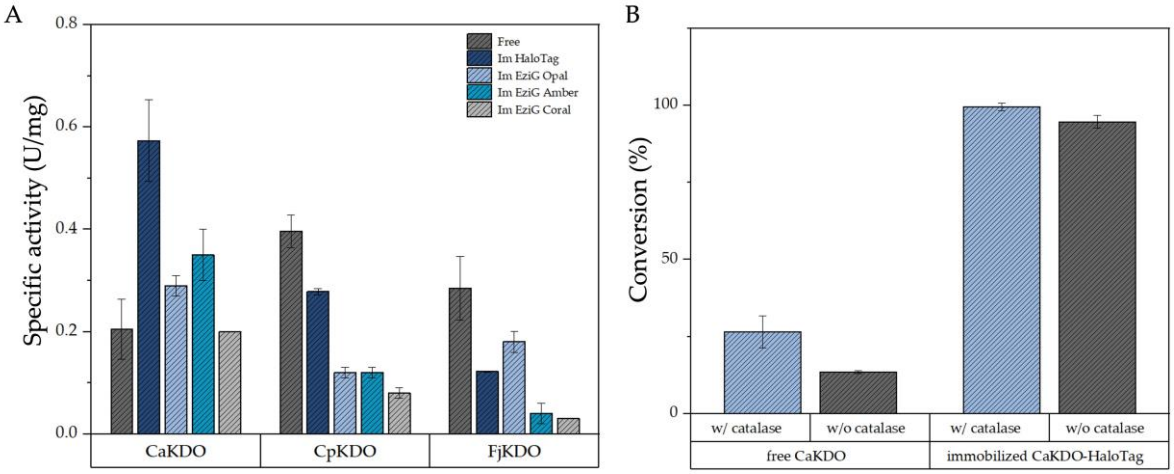

Figure 2. (**A**) Specific activities for L-lysine hydroxylation catalyzed by immobilized KDOs and the respective purified (free) variants with His-Tag. Assays were performed in 1 mL with 200 mM HEPES, pH 7.5, with 0.5 mg mL^{-1} immobilized or free enzyme, 100 mM L-lysine, 150 mM α-KG, 2.5 mM L-ascorbic acid, 0.01 mM DTT, and 1 mM $(NH_4)_2Fe(SO_4)_2$ for 1 h at 25 °C in an overhead shaker. (**B**) Conversion of free *Ca*KDO (with His-Tag) and HaloTag®-immobilized *Ca*KDO with and without 1 mg mL^{-1} catalase after a 24 h reaction time. Assays were performed in 1 mL with the same mixture (see A) on a thermo shaker for 24 h at 21 °C, 750 rpm. Error bars are the result of two technical replicates or, in case of the immobilized variants, of two independent immobilizations.

Since the HaloLink™ resin is commercially available, shows better binding capacities, and for two of the three KDOs, the HaloTag® immobilization worked best, we decided to continue our work with HaloTag®-immobilized KDOs.

While phosphate buffer was used for the purification of the enzymes, HEPES buffer was found to be better suited for biotransformations (data not shown). This is most likely, because the Fe(II) present in the reaction mixture tends to oxidize in aqueous systems. This reaction triggers a reaction called the Fenton reaction, leading to the generation of reactive oxygen species (ROS), which can attack the enzyme and impair its stability. It was shown in previous studies that the amount of formed ROS correlates with the buffer and the pH used and is lower for HEPES buffer in comparison to other buffers [40–42]. Furthermore, buffers such as HEPES and MOPS are more suitable for reaction systems incorporating metal ions due to their lower metal-binding constants compared to other buffers, such as TRIS or phosphate buffers [43]. One way to deal with the generated ROS is to add catalase to the reaction [44]. We tested the addition of catalase exemplarily with both *Ca*KDO preparations, as this enzyme showed the highest activity, but the lowest stability in the free form among

the tested L-lysine hydroxylases (see below). As demonstrated in Figure 2B, catalase was beneficial for the biotransformation with free *Ca*KDO, whereas there was only a negligibly higher conversion for the reaction with HaloTag®-immobilized *Ca*KDO, which does not justify the application of catalase.

Next, we compared the free KDOs with His-Tag to their respective HaloTag® variants immobilized on the HaloLink™ resin in terms of productivity and stability under the reaction conditions (Figure 3). The stabilizing effect of immobilization was most pronounced for *Ca*KDO, where the *Ca*KDO-HaloTag® immobilisate outperformed the free variant already after 1 h of reaction time. While conversion with the free variant stopped after 10%, *Ca*KDO-HaloTag® fully converted 100 mM L-lysine to (3*S*)-hydroxy-L-lysine in 24 h. We could demonstrate that the higher stability was a result of the immobilization and not of the HaloTag® fusion (Supplementary Materials, Figure S9). For *Cp*KDO and *Fj*KDO, both variants, the free and the HaloTag® immobilisate, were stable over the reaction time of 24 h, but reached only 53–79% conversion until the reaction was stopped, which is in line with the lower specific activity of both immobilized enzymes compared to *Ca*KDO-HaloTag® (Figure 2A). As these enzymes are still active after 24 h, full conversion could easily be achieved by a higher enzyme concentration or a prolonged reaction time. The slightly faster conversion observed with free *Cp*KDO and *Fj*KDO relative to the immobilized variants was due to the higher molecular mass of 35 kDa of the HaloTag®-fusions (Figure 3B,C).

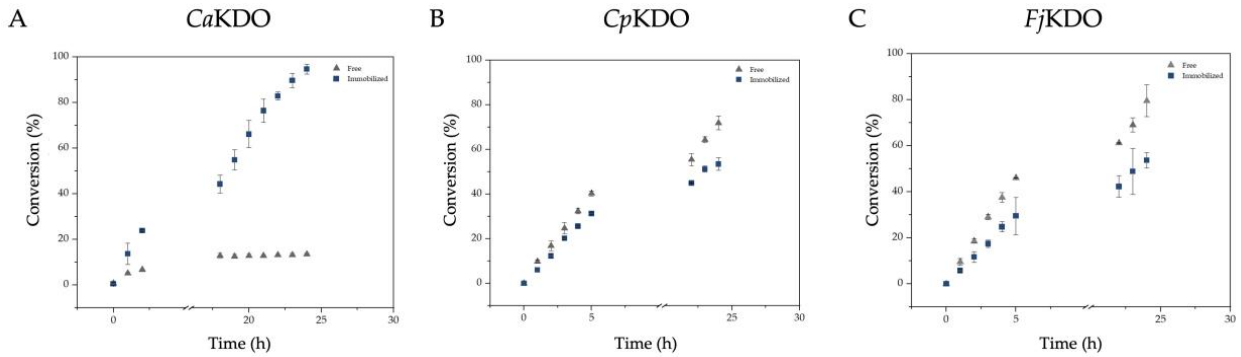

Figure 3. Enzyme stabilities of HaloTag®-immobilized versus free (with His-Tag) KDO variants under the reaction conditions. (**A**) *Ca*KDO-HaloTag® vs free *Ca*KDO (**B**) *Cp*KDO-HaloTag® vs free *Cp*KDO (**C**) *Fj*KDO-HaloTag® vs free *Fj*KDO. Reaction conditions: 200 mM HEPES, pH 7.5, and 0.5 mg mL^{-1} catalyst, 100 mM L-lysine, 150 mM α-KG, 2.5 mM L-ascorbic acid, and 1 mM $(NH_4)_2Fe(SO_4)_2$ for 24 h at 25 °C in an overhead shaker. Reaction volume 1 mL. For further information, see Section 3.3. Error bars are a result of the reaction carried out with two independently immobilized batches.

To maximize the productivity, the L-lysine concentration was increased from 100 mM to 500 mM. Full conversion of 200 mM L-lysine to the corresponding hydroxy-L-lysines was possible with all three KDOs in a 3–4 h reaction time with respectively higher enzyme concentrations of 6.5–7.5 mg mL^{-1} (Figure 4). It is obvious that reactions starting from 200 mM L-lysine proceeded slightly more slowly relative to those with 100 mM, which was probably caused by oxygen limitation, substrate inhibition, or other kinetic effects. The conversion of 500 mM L-lysine was tested with immobilized *Ca*KDO-HaloTag®, which yielded 82% conversion within 26 h (Figure 4A). Aeration in this simple reaction setup using a 5 mL reaction tube attached to an overhead shaker was achieved by opening of the tube every 15 min. The reaction stopped temporarily overnight, due to oxygen depletion, and started again the next day after aeration with the same velocity, as can be deduced from the slope of the conversion curve (Figure 4A). Yet, full conversion of 500 mM L-lysine within about a 12 h reaction time is most probably possible in a reaction setup with continuous aeration, e.g., by performing the reaction in a shaking flask [11,24].

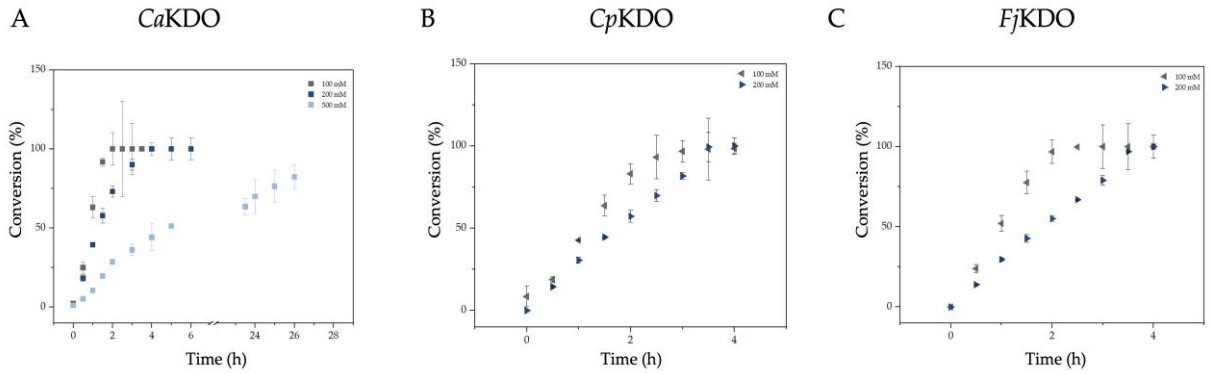

Figure 4. Conversion curves for different L-lysine concentrations (100 mM–500 mM). Reactions were performed in a 1 mL scale in 200 mM HEPES, pH 7.5 with 5 mg mL^{-1} *Ca*KDO (**A**), *Cp*KDO (**B**), and *Fj*KDO (**C**) for 100 mM L-lysine and 7.5 mg mL^{-1} *Ca*KDO, 6.5 mg mL^{-1}, *Cp*KDO, 6 mg mL^{-1} *Fj*KDO for 200 mM L-lysine, respectively. Conversions with 500 mM L-lysine were performed with 5 mg mL^{-1} immobilized *Ca*KDO. The reaction mix contained 100–500 mM L-lysine, 150–750 mM α-KG (1.5 fold excess), 2.5 mM L-ascorbic acid, 0.01 mM DTT, and 1 mM $(NH_4)_2Fe(SO_4)_2$. The reaction was run for 4–26 h at 25 °C in an overhead shaker. Error bars are the result of two independent immobilizations.

2.3. Repetitive Batch Studies

In addition to the benefits immobilization offers on enzyme stabilization, it also enables recycling of the catalyst, which is decisive for the process economy. Recyclability of *Ca*KDO, *Cp*KDO, and *Fj*KDO immobilized via HaloTag® was tested in repetitive batch studies (Figure 5).

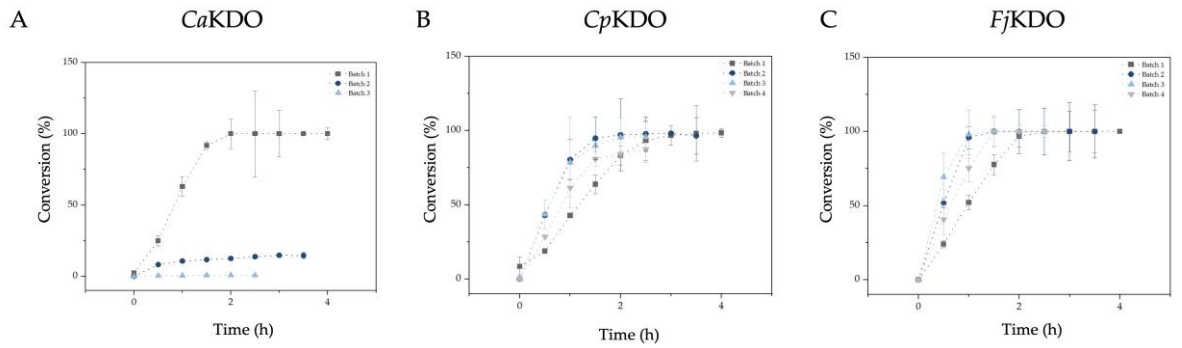

Figure 5. Repetitive batch studies with three HaloTag®-immobilized KDO (**A**) *Ca*KDO (**B**) *Cp*KDO (**C**) *Fj*KDO. Reactions were performed in a 1 mL scale in 200 mM HEPES, pH 7.5, with 5 mg mL^{-1} immobilized enzyme, 100 mM L-lysine, 150 mM α-KG, 2.5 mM L-ascorbic acid, 0.01 mM DTT, and 1 mM $(NH_4)_2Fe(SO_4)_2$ for 24 h at 25 °C in an overhead shaker. After each batch, the immobilized catalyst was precipitated by centrifugation, washed 4 times with 50 mM HEPES, pH 7.5, and stored over night at 4 °C until the next reaction was started with a freshly prepared reaction mixture. Error bars are the result of two independent immobilizations.

After four batches, *Cp*KDO-HaloTag® still gave 84% conversion in 4 h, while *Fj*KDO-HaloTag® converted 100% in 3 h (Figure 5B,C). Even after seven batches, *Fj*KDO-HaloTag® catalyzed the conversion by 27% in 4 h (data not shown). This corresponds to a specific space-time yield of 2333 $g_{product}$ L^{-1} h^{-1} per $g_{immobilized\ CpKDO}$ and 4803 $g_{product}$ L^{-1} h^{-1} per $g_{immobilized\ FjKDO}$. By contrast the single batch reactions gave a space-time yield of 795 $g_{product}$ L^{-1} h^{-1} per $g_{immobilized\ CpKDO}$ and 1081 $g_{product}$ L^{-1} h^{-1} per $g_{immobilized\ FjKDO}$, showing that a recycling approach can effectively increase the reaction efficiency. Factors such as constant shaking, which can lead to friction between the beads and enzyme inactivation, as well as the partial loss of the immobilisate during the washing steps

between batches might lead to the loss of active enzyme. Since the stability of KDOs is a major concern anyway, the little loss of activity after four batches for *Cp*KDO-HaloTag® and after seven batches for *Fj*KDO-HaloTag® exceeded our expectations, especially since previous experiments with SadA immobilized on EziG Amber showed only 10% of the initial reaction rate after the first reaction cycle [28].

Unfortunately, recycling of *Ca*KDO-HaloTag® was not that easy, as the catalyst was already almost inactive after the first batch (Figure 5A). Remarkably, the reaction mix showed a blue color after the first reaction, which occurred after L-lysine was fully consumed (Supplementary Materials, Figure S11). Similar findings were already reported for the 2,4-dichlorophenoxyacetate oxygenase (TfdA) [29,45]. MS-analyses suggested that hydroxylation of a tryptophan residue close to the iron binding site of TfdA occurs in absence of the primary substrate. The tryptophan residue can then chelate the Fe(III) ion located in the active site, which was assumed to be the origin of the blue color. Upon treatment with dithionite, dialysis with EDTA, and reconstitution of Fe(II) in the active site, 81% activity could be restored, most likely due to a displacement of the Fe(III) from the oxidized tryptophan [29,45]. However, in the case of *Ca*KDO, no aromatic residue is close enough to the active site to explain the blue color by an analogous mechanism (Supplementary Materials, Figure S13). Furthermore, in our case, only the reaction mix, not the immobilisate, appeared blue. Since the goal of this work was the application of KDOs in a preparative lab scale, this aspect was not further investigated, but we tested if treatment with dithionite and EDTA could regenerate the activity of the immobilized *Ca*KDO after the first batch. Indeed, it was possible to regain activity, and the regenerated immobilisate was only slightly less active compared to the first batch (Supplementary Materials, Figure S12). These results represent a good basis to regenerate immobilized *Ca*KDO more frequently.

2.4. Preparative Lab-Scale Reactions with CaKDO-HaloTag® and FjKDO-HaloTag®

Next, *Ca*KDO-HaloTag® and *Fj*KDO-HaloTag® were chosen for a reaction on a preparative lab scale for the synthesis of (3*S*)-hydroxy-L-lysine and (4*R*)-hydroxy-L-lysine, respectively. Reaction optimization with free *Ca*KDO at a small scale (1 mL) yielded the optimal reaction parameters (pH, temperature, Fe(II) concentration, use of additives), which were mostly in line with the results already published by Baud et al. [23], for the analytical scale. Only the optimal reaction temperature of the *Ca*KDO reaction was found at 20 °C, whereas the optimal reaction temperature of *Fj*KDO was at 25 °C (data not shown). The optimal reaction parameters were used for both immobilized enzymes to convert 100 mM L-lysine in a 15 mL reaction in non-baffled shaking flasks (Figure 6).

For both reactions, full conversion was reached in less than 24 h, with product titers of 16 g L^{-1} and a total product amount of 240 mg (Figure 6), corresponding to specific space-time yields of 73.4 $g_{product}$ L^{-1} h^{-1} per $g_{immobilized\ CaKDO}$ and 133.65 $g_{product}$ L^{-1} h^{-1} per $g_{immobilized\ FjKDO}$.

In order to increase the scale further, different reaction setups were tested with the immobilized *Ca*KDO-HaloTag®. In a 10 mL shaking flask reaction, full conversion of 200 mM L-lysine was reached in 20 h (Supplementary Materials, Figure S15A) corresponding to a product titer of 32.4 g L^{-1} and a specific space-time yield of 100 g L^{-1} h^{-1} per $g_{immobilized\ CaKDO}$. Continuous aeration was also tested using a synthesis workstation at a 50 mL scale, where full conversion of 100 mM L-lysine was successfully achieved in 70 h (Supplementary Materials, Figure S15B). This corresponds to a product titer of 16.2 g L^{-1}, but a specific space-time yield of only 4.63 g L^{-1} h^{-1} per $g_{immobilized\ CaKDO}$ due to the longer reaction time compared to the shaking flask experiments. Since the aeration rate could not be controlled in our synthesis workstation, we suspected that not only the increased scale, but also an oxygen limitation prolonged the reaction time. We figured out that when working with isolated and immobilized KDOs, the aeration must be carefully balanced. Too little oxygen limits the reaction, but too much oxygen can increase the oxidation of the Fe(II) cofactor, making it either unavailable for the enzyme and/or decreasing the enzyme stability due to the presence of ROS. Often, a simpler setup in shaking flasks can already be

sufficient [11,24]. Here, the filling volume and mixing speed must be assessed to provide adequate oxygen supply. Our results demonstrate that an increase in scale and substrate concentration for KDOs is in general possible using immobilized enzymes in combination with an open reaction system for oxygen supply.

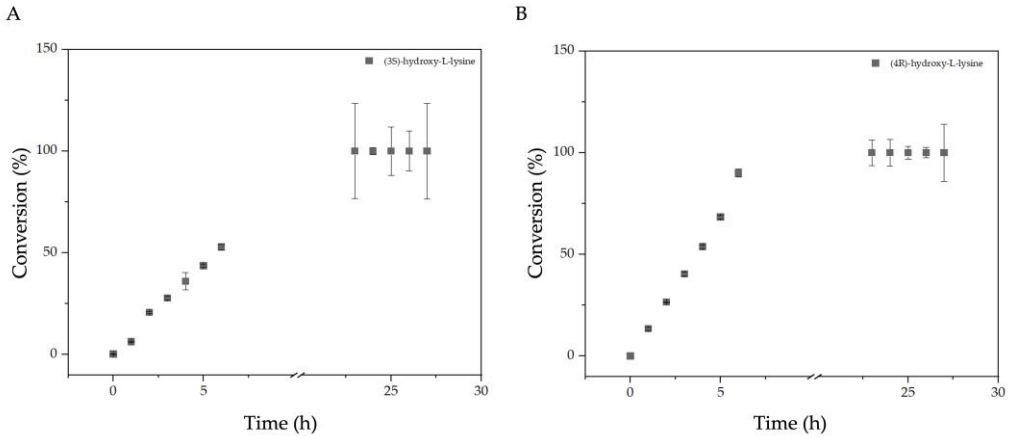

Figure 6. Conversion curves for the synthesis of (3*S*)-hydroxy-L-lysine by *Ca*KDO (**A**) and (4*S*)-hydroxy-L-lysine (*Fj*KDO) (**B**), respectively. Reactions were performed in a 50 mL shaking flask without baffles in a reaction volume of 15 mL, (**A**) 1.3 mg mL^{-1} immobilized *Ca*KDO-HaloTag®, 20 °C, and (**B**) 1.2 mg mL^{-1} immobilized *Fj*KDO-HaloTag®, 25 °C. Reaction mixture: 100 mM L-lysine, 150 mM α-KG, 2.5 mM L-ascorbic acid, 0.01 mM DTT, and 1 mM $(NH_4)_2Fe(SO_4)_2$ for 27 h, at 150 rpm orbital shaking. Error bars are the result of two independent immobilizations.

Different other groups have already worked on the production of hydroxy-L-lysines via a KDO-catalyzed reaction, as summarized in Table 1. Apart from Baud et al. [22,23], who used IMAC-purified enzymes, most groups applied cell-free extracts or whole cells. Working with isolated enzymes resulted in low product titers and total yields (1.6 g L^{-1} or 0.016 g total yields) [22,23]. We were able to increase these titers 10–20-times by increasing the substrate concentration, which was possible due to the optimized production, increased stability, and recyclability by immobilization. Remarkably, our product titers of 32 g L^{-1} (3*S*)-hydroxy-L-lysine are comparable to the product titers of 32.43–43 g L^{-1} obtained with whole cells on a 40 mL scale, as reported by Hara et al. [24].

Table 1. Comparison of process parameters of previously published KDO-catalyzed biotransformations towards hydroxy-L-lysines in a preparative lab scale.

Enzymes	Enzyme Formulation	Product	Reaction Scale (mL)	L-Lysine (mM)	Highest Product Titers (g L^{-1})	Product Titers at Full Conv. (g L^{-1})	Total Yield (g)	Ref.
*Ca*KDO, *Cp*KDO, *Fj*KDO	Isolated enzymes or cell-free extract	(3*S*)-hydroxy-L-lysine (4*R*)-hydroxy-L-lysine	10	10	1.6	1.6	0.016	[22,23]
*Ca*KDO	Cell-free extract	(3*S*)-hydroxy-L-lysine	1000	35	4	4	4	[11]
K3H1 K4H4	Whole cells	(3*S*)-hydroxy-L-lysine (4*R*)-hydroxy-L-lysine	40	500–600 200–400	43 (88% conv.) 86 (88% conv.)	32.43 81.09	3.2–3.44 1.3–1.72	[24]
GlbB	Cell-free extract	(4*R*)-hydroxy-L-lysine	1000	40	6–7 (95% conv.)		6–7	[14]
*Plum*KDO	Whole cells	(4*R*)-hydroxy-L-lysine	50	25–50	4.8 (60% conv.)	4.05	0.20–0.24	[27]
*Ca*KDO *Fj*KDO	HaloTag®-immobilized	(3*S*)-hydroxy-L-lysine (4*R*)-hydroxy-L-lysine	10–50	100–200	16–32 (100% conv.)	32	0.24–0.32	This study

In the context of the preparative synthesis of hydroxy-L-lysines, product isolation must also be considered. The isolation of the target product is easier from less-complex

reaction mixtures, which preferably only contain the target product without residual substrate or side products. The heterogeneity of reaction mixtures is definitely lower in reactions with isolated enzymes instead of cell-free extracts or whole-cell biocatalysts. For the present lysine hydroxylation, separation of hydroxy-L-lysines from residual L-lysine is specifically challenging due to their chemical and physical similarity. Thus, for integrated processes aiming for isolated hydroxy-L-lysines, only processes with full conversion can be considered. In our case, HPLC and GC-ToF-MS analyses demonstrated that the L-lysine was completely converted to the respective hydroxy-L-lysines and contained, besides α-KG, succinate, and HEPES, no further side products (Supplementary Materials, Section S12). With a two-step chromatographic purification [46], the organic acids were fully removed, although traces of HEPES buffer remained, as can be deduced from the NMR-spectra (Supplementary Materials, Figures S27A,B and S32A,B).

2.5. Cascade Reaction towards (2S)-Hydroxy-Cadaverine

As previously shown by Baud et al. [22], coupling of the KDO reaction with a second step incorporating a (lysine) decarboxylase provides access to valuable hydroxycadaverines hydroxylated in the 2- and 3-position depending on the combination of the respective KDOs and lysine decarboxylases (Figure 1). However, the reaction was performed with cell-free extract and limited to a substrate concentration of 10 mM at a 10 mL scale, with the KDO reaction being the limiting step [22]. Because (2*S*)-hydroxy-cadaverine is harder to produce chemically than 3-hydroxy-cadaverine, due to its chiral center, we concentrated on this cascade starting from 100 mM L-lysine in a 15 mL scale with immobilized *Ca*KDO-HaloTag® in the first step and a lysine decarboxylase from *Selenomonas ruminantium* (*Sr*LDC) [22,47,48] in the second reaction step. This pyridoxal phosphate-(PLP)-dependent enzyme accepts besides L-lysine and L-ornithine [49] also (3*S*)-hydroxy-L-lysine as a substrate [22].

Likewise, for *Sr*LDC, we compared the two immobilization techniques: HaloTag® and EziG™, also with the goal of enzyme recycling. Since (3*S*)-hydroxy-L-lysine is not commercially available, all experiments concerning the immobilization, optimization of the reaction conditions, and repetitive batch experiments were carried out with L-lysine as a substrate.

As demonstrated in Figure 7A, soluble and HaloTag®-immobilized *Sr*LDC showed the same performance in the conversion of L-lysine to cadaverine, whereas respective immobilisates on EziG™ beads were less active. The enzyme load of the carrier was higher for the HaloLink™ resin (7.14 mg *Sr*LDC-HaloTag® per mL resin), while the enzyme load of the EziG™ beads was between 0.082 mg per mg EziG™ Opal beads and 0.126 mg per mg EziG™ Coral beads. Similar to the KDOs, *Sr*LDC binds better to the HaloLink™ resin, showing a similar specific activity as the free enzyme, as can be deduced from the conversion curve (Figure 7A).

Next, the HaloTag®-immobilized *Sr*LDC was tested for its activity towards the different substrates (L-lysine, L-ornithine, (3*S*)-hydroxy-L-lysine). After a 5 h reaction time, almost full conversion of the substrate L-lysine (100 mM) was achieved, whereas the conversion of L-ornithine and (3*S*)-hydroxy-L-lysine occurred significantly more slowly (Figure 7B). Yet, full conversion of L-ornithine to putrescin was achieved after 72 h. At this point, only 11% of (3*S*)-hydroxy-L-lysine was converted to (2*S*)-hydroxy-cadaverine, showing the low activity of *Sr*LDC for this substrate. However, it has to be considered that (3*S*)-hydroxy-L-lysine was applied in the form of a supernatant taken from a previous KDO reaction. Therefore, other components in the reaction mixture might also lead to a decrease in activity.

Simultaneously, important reaction parameters for the *Sr*LDC-HaloTag® reaction from L-lysine to cadaverine were investigated. The influence of pH, substrate concentration, temperature, and the concentration of the cofactor PLP on the reaction was tested (Supplementary Materials, Section S7).

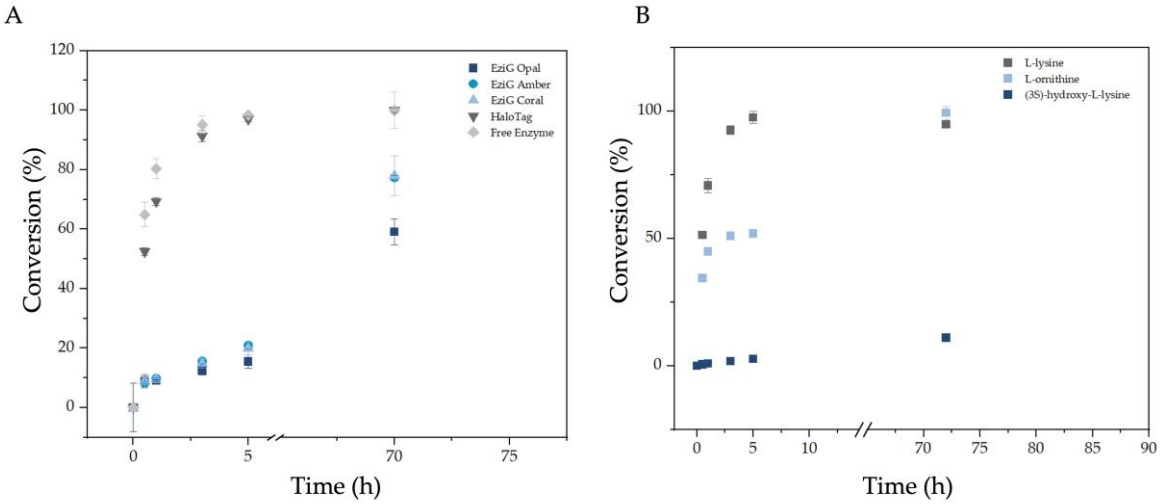

Figure 7. (**A**) Comparison of the conversion of free *Sr*LDC (with His-Tag), *Sr*LDC HaloTag®-immobilized to HaloLink™ resin, and *Sr*LDC immobilized to EziG™ Opal, Amber, and Coral. (**B**) Comparison of the conversion of L-lysine, L-ornithine, and (3*S*)-hydroxy-L-lysine with immobilized *Sr*LDC-HaloTag® (0.1 mg mL^{-1}). Reaction conditions: volume: 1 mL, 100 mM L-lysine or L-ornithine, 2 mM PLP in 100 mM HEPES, pH 7.0, in an overhead shaker at 35 °C under the exclusion of light. For (3*S*)-hydroxy-L-lysine, the supernatant of the *Ca*KDO reaction was used (Figure 6A). Error bars are a result of two technical replicates or, in the case of the immobilized variants, of two independent immobilizations.

The highest cadaverine concentration after 5 h (67.87 ± 2.72%) was obtained starting from 100 mM L-lysine, whereas L-lysine concentrations > 100 mM resulted in lower conversion, which could be explained by possible substrate inhibition of the enzyme (Supplementary Materials, Figure S16C). In short-term experiments (20 min), the tested PLP concentrations in the range of 0.05–2 mM gave identical results (Supplementary Materials, Figure S16B). Since supplementation of PLP is known to be beneficial for LDCs and the cofactor is unstable at room temperature and towards light exposure [50], 1 mM PLP was used for further experiments. Additionally, a pH of 7 and a reaction temperature of 35 °C were found to be optimal (Supplementary Materials, Section S7, Figure S16A,D).

Under optimized reaction conditions, the sequential cascade reaction was performed without intermediate purification (Figure 8A). Full conversion of 100 mM L-lysine in the first reaction step was achieved after approximately a 10 h reaction time in a shaking flask. After 25 h, the supernatant containing the (3*S*)-hydroxy-L-lysine was transferred to a falcon tube, and 2.5 mg mL^{-1} of immobilized *Sr*LDC was added. After 47 h, a conversion of 97% was reached, corresponding to a specific space-time yield of 6.5 g L^{-1} h^{-1} per $g_{immobilized\ SrLDC}$ and a product titer of 11.6 g L^{-1} (2*S*)-hydroxy cadaverine. The results demonstrate that the *Sr*LDC reaction is not impaired by components from the KDO-catalyzed step, since increasing the enzyme concentration from 0.1 mg mL^{-1} to 2.5 mg mL^{-1} led to full conversion of (3*S*)-hydroxy-L-lysine to (2*S*)-hydroxy-cadaverine. Increased enzyme concentrations could principally decrease the reaction time for both steps further.

HPLC and GC-ToF-MS analyses demonstrated full conversion of the (3*S*)-hydroxy-L-lysine to (2*S*)-hydroxy-cadaverine (Supplementary Materials, Section S12), which enabled us to successfully purify the (2*S*)-hydroxy-cadaverine by a protocol from Fossey-Jouenne et al. [46] for NMR analysis (Supplementary Materials, Section S12) without any remaining impurities (Figure S41A,B). This is in contrast to in vivo approaches with a *Corynebacterium glutamicum* strain overexpressing recombinant KDO genes and three different LDC genes for the production of (4*R*)-hydroxy-L-lysine and 3-hydroxy-cadaverine from L-lysine [21].

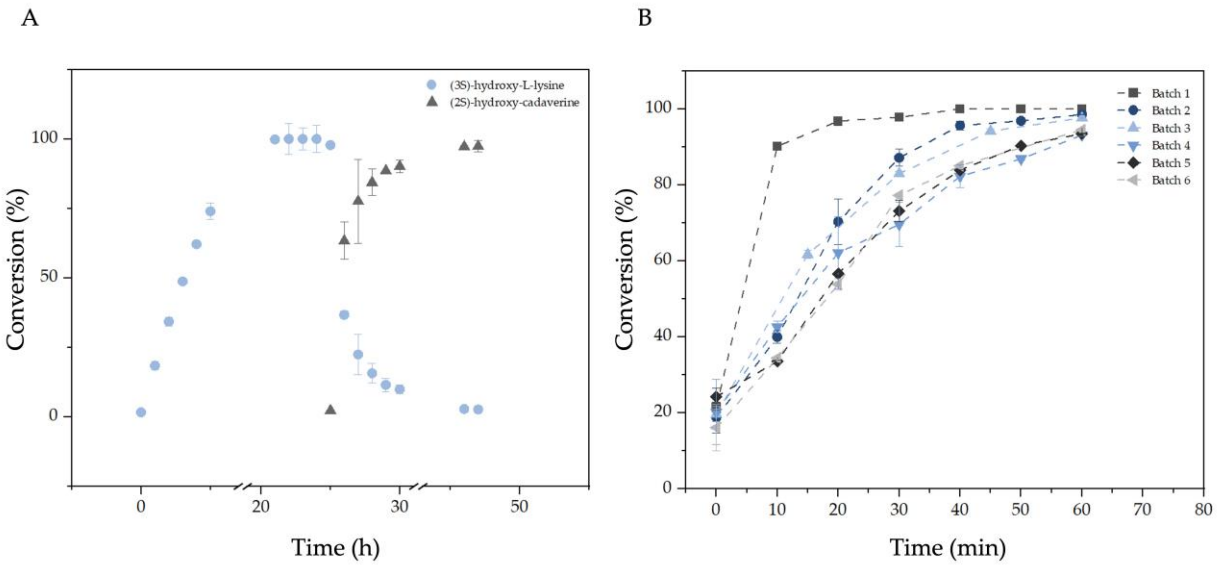

Figure 8. Two-step cascade reaction towards (2*S*)-hydroxy-cadaverine using *Ca*KDO-HaloTag® and *Sr*LDC-HaloTag® and repetitive batch experiments of *Sr*LDC-HaloTag® for the production of cadaverine. (**A**) Conversion curves of the sequential cascade reaction of immobilized *Ca*KDO and *Sr*LDC in preparative scale. The KDO reaction was performed in a 50 mL shaking flask without baffles in a reaction volume of 15 mL, at 20 °C, and 1.3 mg mL^{-1} HaloTag®-immobilized *Ca*KDO. Reaction conditions: 100 mM L-lysine, 150 mM α-KG, 2.5 mM L-ascorbic acid, 0.01 mM DTT, and 1 mM $(NH_4)_2Fe(SO_4)_2$ for 25 h, at 150 rpm orbital shaking. Afterwards, the reaction supernatant was transferred to a 50 mL falcon tube; the pH was titrated to 7.0; 1 mM PLP was added. The second reaction was started with 2.5 mg mL^{-1} HaloTag®-immobilized *Sr*LDC. The reaction was run for another 22 h in an overhead shaker at 35 °C under the exclusion of light. (**B**) Repetitive batch reactions of HaloTag®-immobilized *Sr*LDC. Reaction was performed in a 50 mL falcon tube, in a reaction volume of 15 mL and 1 mg mL^{-1} HaloTag®-immobilized *Sr*LDC starting from 100 mM L-lysine, in 100 mM HEPES, pH 7.0, with 1 mM PLP in an overhead shaker at 35 °C under exclusion of light. After each batch, the immobilized catalyst was separated by centrifugation, washed 4 times with 100 mM HEPES, pH 7.0, and used for the next reaction. Error bars are the result of two independent immobilizations.

Similar product titers for 3-hydroxy-cadaverine (11.4 g/L) to our approach for the production of (2*S*)-hydroxy-cadaverine could be achieved, with a strain containing *Fj*KDO and LDCc. However, the amount of by-product (cadaverine titer 39 g L^{-1}) and intermediates ((4*R*)-hydroxy-L-lysine titer 4.1 g L^{-1}) was high, most likely due to the substrate preference of the lysine decarboxylases for L-lysine and the generally lower activity of LDCs towards the hydroxy-L-lysines. While the constant supply of L-lysine and α-KG provided by the cellular metabolism in vivo is certainly advantageous, the pH inside living cells is hard to control relative to isolated enzymes, especially when pH-active compounds (lysine and cadaverine derivatives) are involved and cascade reactions include enzymes that are highly pH dependent [48,51]. Further, isolation of the target product 3-hydroxy-cadaverine from a mixture of substrate (L-lysine), intermediate ((4*R*)-hydroxy-L-lysine), by-product (cadaverine), and other cellular components is definitely challenging, due to the close physical and chemical properties of the molecules. Thus, in the case of cascades containing KDOs and LDCs, a sequential approach including isolated immobilized enzymes seems to be advantageous and simpler compared to in vivo approaches.

Next, we investigated if immobilized *Sr*LDC-HaloTag® could be recycled in repetitive batch experiments using L-lysine (100 mM) as a substrate (Figure 8B). It can be clearly seen that the first reaction is the fastest and the turnover rates decrease less between the second and the last reaction (cycles 2–6) than between cycle 1 and 2. Still, a conversion of $\geq$ 94% could be achieved in the last cycle after 1 h. So far, immobilized *Sr*LDC-HaloTag® showed

a reusability of at least six cycles in a 15 mL scale with little loss of activity and potentially even a higher number of cycles. This is a good basis for further reaction engineering of the cascade towards (2*S*)-hydroxy cadaverine. Because the enzyme activity towards (3*S*)-hydroxy-L-lysine is much lower than towards L-lysine, prolonged reaction times are necessary to achieve full conversion.

Besides, the product of the decarboxylation of L-lysine, cadaverine, is also an interesting industrial compound for the production of fully biobased polymers [15,52]. Biological production of cadaverine is commonly performed by fermentative microbial production [52], (immobilized) whole recombinant *E. coli* cells [15,53], or immobilized LDCs. Immobilization of LDCs was previously performed on poly(3-hydroxybutyrate) (P(3HB) biopolymers [54], chitin [55], or via different carrier-free immobilization methods, such as catalytically active inclusion bodies (CatIBs) [56], or in the form of crosslinked enzyme aggregates (CLEASs) [57]. Currently, most processes using immobilized enzymes use the constitutive (*Ec*LDCc) or inducible (CadA) LDCs from *E. coli*. While CadA is active in a pH range between 5 and 6, it is rapidly inhibited at pH higher that 8.0 [58]. Furthermore, it is inhibited at higher concentrations of lysine [59] and cadaverine [60]. In contrast, the constitutive *Ec*LDCc has a broader pH range [51] and is hardly inhibited by L-lysine [61]. To our knowledge, an application of *Sr*LDC for the production of cadaverine has not yet been tested. As was recently extensively reviewed by Huang et al. [15], biological cadaverine production using fermentation, whole cells, and biotransformations with immobilized enzymes led to space-time yields between 10 g L^{-1} h^{-1} and 204 g L^{-1} h^{-1}. With HaloTag®-immobilized *Sr*LDC, we achieved a product titer of 58.4 g L^{-1}, corresponding to a specific space-time yield of 655 g L^{-1} h^{-1} per g $_{\text{immobilized } SrLDC}$. Furthermore, HaloTag®-immobilized *Sr*LDC was able to catalyze the full conversion of 100 mM L-ornithine on a 15 mL preparative lab reaction (Supplementary Materials, Figure S17), giving access to 8.8 g L^{-1} 1,4-diaminobutane (putrescine), which is another interesting building block for the production of biobased polyamides [16].

Considering all these factors, *Sr*LDC is an interesting enzyme for further investigation of its potential for the synthesis of cadaverine, putrescine, and respective hydroxylated derivatives.

3. Materials and Methods

3.1. Materials

All chemicals were purchased from Sigma-Aldrich, Roth, Merck, VWR International (Radnor, PA, USA), Merck KGaA (Darmstadt, Germany), Sigma-Aldrich Chemie GmbH (Steinheim, Germany), AppliChem GmbH (Darmstadt, Germany), and Thermo Fisher Scientific (Waltham, MA, USA). Plasmid pGro7 (GroEL/GroES) was obtained from Takara Holdings. The strains used were *Escherichia coli* DH5α and *Escherichia coli* BL21 (DE3). The plasmids pET-22b(+)-*Ca*KDO, pET-22b(+)-*Cp*KDO, pET-22b(+)-*Fj*KDO, and pET-22b(+)-*Sr*LDC were a kind gift from Prof. Anne Zaparucha and were described previously [22,23].

HaloLink™ resin was purchased from Promega. EziG™ immobilization particles were kindly provided by Dr. Karim Engelmark Cassimjee.

3.2. Immobilization of KDOs and SrLDC on HaloTag® and EziG™

A 15% (*w/v*) (*Sr*LDC) or 30% (*w/v*) (KDO) cell suspension consisting of the produced pellet and HaloTag® immobilization buffer (KDOs: 50 mM HEPES, pH 7.5 with 10% glycerol, *Sr*LDC: 100 mM HEPES, pH 7.0 with 10% glycerol) or EziG™ immobilization buffer (20 mM HEPES, pH 7.5 (KDOs) or pH 7.0 (*Sr*LDC), with 500 mM NaCl) was prepared from the frozen *E. coli* cell pellets. The mixture was suspended in an ice bath for 30 min under constant magnetic stirring. Cells were lysed by sonication and debris removed by centrifugation. Afterwards, 1 mL of the cell-free extract was added to 1 mL washed (with HaloTag® buffer) HaloLink™ slurry (25% beads) or 10 mg EziG™ beads (Amber, Coral, Opal) and incubated at 25 °C for 30 min in an overhead shaker. After incubation, the immobilisates were washed 4 times with 50 mM HEPES, pH 7.5 (KDOs), or 100 mM

HEPES, pH 7.0 (*Sr*LDC), and the amount of bound protein was quantified by the BCA assay (Supplementary Materials, Section S3.1.1) and confirmed by SDS PAGE (Supplementary Materials, Section S3.1.2).

3.3. Biotransformation with KDOs

All reactions were performed as technical duplicates (same enzyme batch). The 10 µL samples were diluted 1:50 with 50 mM HEPES buffer, and the reaction was stopped by incubation at 80 °C for 5 min in a thermo shaker (Eppendorf). Substrate and product concentrations were determined by HPLC (3.6). Reaction mix: 100–500 mM L-lysine, 150–1000 mM α-KG (1.5 molar excess), 1 mM ammonium iron(II)sulfate, 2.5 mM L-ascorbic acid, 0.01 mM DTT in 200 mM HEPES buffer, pH 7.5.

3.3.1. Initial Rate Activity

For initial activity measurements, enzyme concentrations of 0.5–1 mg mL^{-1} for the free and immobilized variants of *Ca*KDO, *Cp*KDO, and *Fj*KDO were used. Conversions were measured up to a maximum of 10% to ensure initial rate conditions. Due to the different residual activities of the immobilized enzymes, the assay conditions were respectively adapted to the enzyme preparation (Table 2).

Table 2. Assay conditions for respective enzymes and formulations.

Enzyme Formulation	Reaction Time	Sampling (10 µL)
*Ca*KDO EziG™	60 min	every 10 min
*Ca*KDO HaloTag®	20 min	every 4 min
*Cp*KDO HaloTag®& EziG™ *Fj*KDO HaloTag®& EziG	50 min	every 10 min
Free enzymes	30 min	every 5 min

The reaction was mixed at 25 °C in an overhead shaker for sufficient mixing of the beads and the reaction mixture

3.3.2. Analytical Scale Reactions

For analytical-scale reactions and initial rate activity measurements, the reaction was started by adding 1 mL reaction mix (3.3) to a 2 mL reaction tube containing either the lyophilized free enzyme or the immobilized enzyme. The reaction was mixed at 25 °C in an overhead shaker or vertically attached on a thermomixer to guarantee sufficient mixing of the beads and the reaction mixture.

Enzyme formulations and concentrations for different experiments:

Stability under reaction conditions: 0.5 mg mL^{-1} for the free and immobilized variants.

Different substrate concentrations:

HaloTag® variants immobilized on HaloLink™ resin:

- 5 mg mL^{-1} *Ca*KDO, *Cp*KDO, *Fj*KDO for 100 mM L-lysine;
- 7.5 mg mL^{-1} *Ca*KDO 6.5 mg mL^{-1} *Cp*KDO 6 mg mL^{-1} *Fj*KDO for 200 mM L-lysine;
- 5 mg mL^{-1} CaKDO for 500 mM L-lysine.

3.3.3. Repetitive Batch Experiments

For repetitive experiments, 1 mL of the reaction mixture (3.3) was added to the immobilized enzyme (5 mg mL^{-1} *Ca*KDO-HaloTag®, *Cp*KDO-HaloTag®, *Fj*KDO-HaloTag®) using 5 mL reaction tubes. In order to guarantee sufficient oxygen supply, the tubes were opened every 15 min. Samples (10 µL) were taken every 30 min over a period of 4 h for subsequent HPLC analysis. Afterwards the tubes were centrifuged, the beads were washed 4 times with 1 mL 50 mM HEPES buffer, pH 7.5, and stored overnight at 4 °C. The next day, the beads were washed once with 200 mM HEPES buffer, pH 7.5, before the reaction was

started again with a freshly prepared reaction mixture. The procedure was repeated for three to seven batches, depending on the enzyme.

3.3.4. Regeneration of Immobilized *Ca*KDO-HaloTag®

After the first batch (3.3, 3.3.3), the beads were washed 4 times with 50 mM HEPES buffer, pH 7.5. After the addition of different concentrations of dithionite (1 or 10 mM) and 100 mM EDTA, the beads were shaken in an overhead shaker for 1 h at room temperature. Afterwards, the tubes were centrifuged; the beads were washed 4 times with 50 mM HEPES buffer, pH 7.5, to remove EDTA and dithionite and stored overnight at 4 °C. The next day, the beads were washed once with 200 mM HEPES buffer, pH 7.5, and the reaction was started again with a freshly prepared reaction mixture including 1 mM $Fe(NH_4)_2(SO_4)_2$, thereby restoring the cofactor for the reaction. As a control, one of the reactions was incubated only with 50 mM HEPES (Supplementary Materials, Figure S12D).

3.3.5. Reactions in Preparative Lab Scale

Conversion of 100 mM L-lysine in 15 mL: The reaction was started by adding 15 mL of reaction mix (3.3) with 100 mM L-lysine to a 50 mL Erlenmeyer flask without baffles containing 1.2 mg mL^{-1} and 1.3 mg mL^{-1} HaloTag®-immobilized *Ca*KDO and *Fj*KDO, respectively. The reaction was mixed by orbital shaking at 150 rpm at 20 °C and 25 °C for *Ca*KDO and *Fj*KDO, respectively. Each reaction was performed as a technical duplicate. Samples (10 µL) were taken every hour over a period of 24 h. The reaction was quenched by heat inactivation at 80 °C for 5 min. Substrate and product concentrations were measured by HPLC (3.6).

Conversion of 200 mM L-lysine in 10 mL: The reaction was started by adding 10 mL of reaction mix (3.3) with 200 mM L-lysine and 1 mg mL^{-1} catalase (Sigma Aldrich) to a 25 mL Erlenmeyer flask without baffles containing 1.35 mg mL^{-1} HaloTag®-immobilized *Ca*KDO. The reaction was mixed by orbital shaking at 150 rpm at 20 °C. Samples were taken every hour over a period of 52 h, excluding night hours. For sample workup and analysis, see above.

Conversion of 100 mM L-lysine in 50 mL using an EasyMax 402 Thermostat system (Mettler Toledo): The reaction was started by adding 30 mL of reaction mix (3.3) to the EasyMax reaction vessel (100 mL) containing 20 mL immobilized *Ca*KDO HaloTag® slurry (1 mg/mL enzyme) in 200 mM HEPES, pH 7.5. The reaction was stirred at 150 rpm, 20 °C, and the pH was continuously controlled with 0.5 M NaOH, while filtered purge gas was introduced to the surface of the reaction and incorporated into the reaction mixture by stirring (the aeration rate cannot be controlled with this device). Samples were taken every hour over a period of 70 h, excluding night hours. For sample workup and analysis, see above.

3.4. Biotransformations with SrLDC

All reactions were mixed at 35 °C in an overhead shaker to guarantee sufficient mixing of the beads and the reaction mixture. Reactions were performed as technical duplicates (same enzyme batch). The 10 µL samples were diluted 1:50 with 50 mM HEPES buffer, and the reaction was stopped by incubation at 80 °C for 5 min in a thermo shaker (Eppendorf). Substrate and product concentrations were determined by HPLC (3.6).

3.4.1. Analytical Scale

The reaction was started by adding 1 mL reaction mix containing 100 mM L-lysine, 1 mM PLP, and 100 mM HEPES buffer, pH 7.0, to a 2 mL reaction tube containing either the lyophilized free enzyme or immobilized enzyme. In the case of experiments with (3*S*)-hydroxy-L-lysine, the reaction supernatant from the previous KDO reaction was taken, and 1 mM PLP was added and titrated to pH 7.0.

3.4.2. Repetitive Batch Experiments in a Preparative Lab Scale

For repetitive experiments, 15 mL of the reaction mixture (100 mM L-lysine, 1 mM PLP in 100 mM HEPES, pH 7.0) was added to the 1 mg mL^{-1} immobilized enzyme. The reaction was performed in 50 mL falcon tubes. Samples were taken every 10 min over a period of 1 h. Afterwards, the tubes were centrifuged, washed 2× with 100 mM HEPES buffer, pH 7.0, and used for the next batch. The procedure was repeated for 6 batches.

3.4.3. *Ca*KDO and SrLDC Cascade Reaction

The *Ca*KDO-HaloTag® reaction was performed in a 50 mL shaking flask without baffles in a reaction volume of 15 mL, at 20 °C, and 1.3 mg mL^{-1} *Ca*KDO-HaloTag® immobilized on HaloLink™ resin. The reaction mix contained 100 mM L-lysine, 150 mM α-KG, 2.5 mM L-ascorbic acid, 0.01 mM DTT, 1 mM $(NH_4)_2Fe(SO_4)_2$, and 200 mM HEPES, pH 7.5. The reaction was performed for 27 h, at 150 rpm orbital shaking. Afterwards, the reaction supernatant (consisting of approximately 100 mM (3*S*)-hydroxy-L-lysine, 50 mM α-KG, 100 mM succinate, 2.5 mM L-ascorbic acid, 0.01 mM DTT, 1 mM $(NH_4)_2Fe(SO_4)_2$, 200 mM HEPES, pH 7.5) was transferred to a 50 mL falcon tube; the pH was titrated to 7.0, and 1 mM PLP was added. The second reaction was started by adding 2.5 mg mL^{-1} *Sr*LDC-HaloTag® immobilized on HaloLink™ resin and run for another 21 h in an overhead shaker at 35 °C under the exclusion of light. Samples (10 µL) were taken every hour (excluding night hours) and analyzed by HPLC (3.6).

3.5. Product Purification

Hydroxy-L-lysines and (2*S*)-hydroxy-cadaverine were purified as previously described by Fossey-Jouenne et al. [46].

3.6. HPLC Analyses

All biotransformations were monitored by HPLC using a diode array detector (DAD) or a fluorescence detector (FLD), with the DAD detector giving the best results. For the analysis of amino acid derivatives, diamines, and (2*S*)-hydroxy-cadaverine, a pre-column derivatization step with *ortho*-phthaldialdehyde (OPA, Sigma-Aldrich) was performed. Approximate retention times were 5.6 min for L-histidine (internal standard), 8.8 min for 5-hydroxy-(D,L)-lysine, 8.9 min for (4*S*)-hydroxy-L-lysine, 9.0 min for (3*S*)-hydroxy-L-lysine, 9.1 min for L-lysine, 9.4 min for (2*S*)-hydroxy-cadaverine, and 10.0 min for cadaverine. Concentrations were derived from the linear calibration of five reference solutions (0.1–2.5 mM) containing L-histidine, 5-hydroxy-(D,L)-lysine, L-lysine, and cadaverine. Calibration was performed at least once per week or prior to every HPLC run. For details and chromatograms, see Supplementary Materials, Sections S9 and S12.

3.7. GC-ToF-MS Analysis

Components of the reaction mixture and mass information to identify the different hydroxy-L-lysines and the (2*S*)-hydroxy-cadaverine were analyzed by GC-ToF-MS according to a previously described protocol [62]. For details, see Supplementary Materials, Section S11.

(3*S*)-hydroxy-L-lysine, (4*R*)-hydroxy-L-lysine, and 5-hydroxy-(D,L)-lysine gave two trimethyl-silyl (TMS) derivatives modified with four and five TMS groups, respectively. On the GC chromatogram (Supplementary Materials, Figure S20), we can clearly identify these derivatives by retention times and masses (Supplementary Materials, Figure S20, Table S5). GC-ToF-MS analytics was also able to discriminate between the two possible diastereomers. As can be seen in the GC-chromatogram (Supplementary Materials, Figure S20), both TMS species of 5-hydroxy-(D,L)-lysine, which was bought as a diastereomeric mixture, showed double peaks, indicating the presence of diastereomers, while the respective TMS derivatives of (3*S*)-hydroxy-L-lysine, (4*R*)-hydroxy-L-lysine, and (2*S*)-hydroxy-cadaverine only showed single peaks, indicating the presence of only one diastereomer.

3.8. NMR Analysis

After product purification (3.5) of the respective hydroxy-L-lysines and the (2*S*)-hydroxy-cadaverine, the 1D and 2D NMR spectra were recorded. For both components, the NMR signals were successfully assigned to the molecular structure (Supplementary Materials, Section S12). While no major impurities were visible in the (2*S*)-cadaverine spectrum (Supplementary Materials, Figure S42A,B), some impurities remained in the hydroxyl-lysine samples, probably due to the high concentration of HEPES buffer present in the reaction supernatant (Supplementary Materials, Figures S27A,B and S32A,B). For both hydroxyl-L-lysine derivatives, the position of the hydroxyl group was assigned indirectly through the CH-group, as hydroxyl groups are not visible in the NMR spectrum in deuterated water (Supplementary Materials, Figures S27A,B and S32A,B).

4. Conclusions

Here, we demonstrate that covalent in situ immobilization is an appropriate tool to access the preparative potential of KDOs. Immobilization via the HaloTag® solved almost all the problems that hamper the application of KDOs besides the analytical scale. The one-step immobilization rapidly concentrated the enzyme from cell-free extracts on the carrier with high residual activity and improved stability, specifically in the case of *Ca*KDO, which showed the lowest stability among the tested KDOs. Upon KDO immobilization, the increase in the stability enabled a substrate conversion of >200 mM L-lysine, without the generation of any side products. Further, enzyme recycling was demonstrated, which was simple for immobilized *Cp*KDO-HaloTag® and *Fj*KDO-HaloTag®, but required treatment with dithionite and EDTA in the case of *Ca*KDO. We were able to apply the immobilized *Ca*KDO-HaloTag® and *Fj*KDO-HaloTag® in a preparative lab scale (15 mL) and could show that a further increase in scale (up to 50 mL) or substrate concentration (200 mM L-lysine) was in general possible.

This generally led to a decrease in process costs and an increase in process sustainability, meeting the requirements of processes that will become increasingly important within the next few years.

Especially in the cascade reactions of KDOs and LDCs towards hydroxy-cadaverine derivatives, the immobilization approach seems to be superior to systems using in vivo two-phase fermentation approaches [21]. In the case of cascade reactions where the second enzyme has a higher activity towards the substrate of the first reaction (L-lysine) than the intermediate (hydroxyl-L-lysine), full conversion in the KDO-catalyzed step is mandatory, before the LDC comes into play to avoid the loss of L-lysine by the production of cadaverine as a main side product and related purification problems. Using immobilized enzymes allows for an easy separation of the enzyme in a simple sequential reaction setup, where the reaction parameters of the different reaction steps can easily be adjusted to the respective optimal parameters (temperature, pH, reactor design, aeration, and mixing of immobilized enzymes) and successful product purification.

We propose that covalent in situ immobilization is an appropriate tool to access the preparative potential of many other KDOs.

Supplementary Materials: The following supporting information can be downloaded at: https://www.mdpi.com/article/10.3390/catal12040354/s1 [63,64].

Author Contributions: Conceptualization, S.S. and M.P.; methodology, S.S., L.A., J.G., M.B., S.W. and M.P.; validation, S.S., L.A., J.G., M.B., S.W. and M.P.; formal analysis, S.S., L.A., J.G., M.B., S.W. and M.P.; investigation, S.S., L.A., J.G., M.B. and S.W.; resources, M.P.; data curation, M.P.; writing—original draft preparation, S.S.; writing—review and editing, M.P.; visualization, S.S.; supervision, M.P.; project administration, M.P.; funding acquisition, M.P. All authors have read and agreed to the published version of the manuscript.

Funding: This research was supported by the CLIB-Competence Center Biotechnology (CKB) funded by the European Regional Development Fund (EFRE) and the North-Rhine Westphalian Ministry of

Economic Affairs, Innovation, Digitalization and Energy (MWIDE) (grant number: EFRE-0300097). Funded by the Deutsche Forschungsgemeinschaft (DFG, German Research Foundation): 491111487.

Data Availability Statement: The data are contained within the article or Supplementary Materials.

Acknowledgments: The plasmids pET-22b(+)-*Ca*KDO, pET-22b(+)-*Cp*KDO, pET-22b(+)-*Fj*KDO, and pET-22b(+)-*Sr*LDC and the standards of (3*S*)-hydroxy-L-lysine and (4*R*)-hydroxy-L-lysine were a kind gift from Anne Zaparucha. We further thank Anne for many fruitful discussions and helpful advice. Furthermore, we thank Christiane Claaßen for the analysis of the NMR spectra, Philipp Nerke for scientific advice and fruitful discussions, and Astrid Wirtz for her help concerning HPLC analytics. Many thanks also go to members of the IBOC team for performing NMR measurements and Karim Engelmark Cassimjee for providing the EziG™ immobilization particles.

Conflicts of Interest: The authors declare no conflict of interest.

References

1. Turner, N.J.; Humphreys, L. *Biocatalysis in Organic Synthesis: The Retrosynthesis Approach*; The Royal Society of Chemistry: London, UK, 2018; ISBN 978-1-78262-530-8.
2. Bernhardt, R.; Urlacher, V.B. Cytochromes P450 as promising catalysts for biotechnological application: Chances and limitations. *Appl. Microbiol. Biotechnol.* **2014**, *98*, 6185–6203. [CrossRef] [PubMed]
3. O'Reilly, E.; Köhler, V.; Flitsch, S.L. Cytochromes P450 as useful biocatalysts: Addressing the limitations. *Chem. Commun.* **2011**, *47*, 2490–2501. [CrossRef]
4. Gao, S.S.; Naowarojna, N.; Cheng, R.; Liu, X.; Liu, P. Recent examples of α-ketoglutarate-dependent mononuclear non-haem iron enzymes in natural product biosyntheses. *Nat. Prod. Rep.* **2018**, *35*, 792–837. [CrossRef] [PubMed]
5. Martinez, S.; Hausinger, R.P. Catalytic mechanisms of Fe(II)- and 2-Oxoglutarate-dependent oxygenases. *J. Biol. Chem.* **2015**, *290*, 20702–20711. [CrossRef] [PubMed]
6. Schofield, C.; Hausinger, R. 2-Oxoglutarate-Dependent Oxygenases. In *Metallobiology*; Schofield, C., Hausinger, R., Eds.; The Royal Society of Chemistry: London, UK, 2015; ISBN 978-1-84973-950-4.
7. Peters, C.; Buller, R.M. Industrial application of 2-oxoglutarate-dependent oxygenases. *Catalysts* **2019**, *9*, 221. [CrossRef]
8. Hibi, M.; Ogawa, J. Characteristics and biotechnology applications of aliphatic amino acid hydroxylases belonging to the Fe(II)/α-ketoglutarate-dependent dioxygenase superfamily. *Appl. Microbiol. Biotechnol.* **2014**, *98*, 3869–3876. [CrossRef] [PubMed]
9. Wang, F.; Zhu, M.; Song, Z.; Li, C.; Wang, Y.; Zhu, Z.; Sun, D.; Lu, F.; Qin, H.M. Reshaping the Binding Pocket of Lysine Hydroxylase for Enhanced Activity. *ACS Catal.* **2020**, *10*, 13946–13956. [CrossRef]
10. Marin, J.; Didierjean, C.; Aubry, A.; Casimir, J.; Briand, J.; Guichard, G.; Poincare, H. Synthesis of Enantiopure 4-Hydroxypipecolate and 4-Hydroxylysine Derivatives from a Common 4,6-Dioxopiperidinecarboxylate Precursor. *J. Org. Chem.* **2004**, *69*, 130–141. [CrossRef]
11. Zhang, X.; King-Smith, E.; Renata, H. Total Synthesis of Tambromycin by Combining Chemocatalytic and Biocatalytic C−H Functionalization. *Angew. Chem. Int. Ed.* **2018**, *57*, 5037–5041. [CrossRef]
12. Lampe, J.W.; Hughes, P.F.; Biggers, C.K.; Smith, S.H.; Hu, H. Total Synthesis of (−)- and (+) Balanol. *Synthesis* **1996**, *3263*, 4572–4581. [CrossRef]
13. Amatuni, A.; Renata, H. Identification of a lysine 4-hydroxylase from the glidobactin biosynthesis and evaluation of its biocatalytic potential. *Org. Biomol. Chem.* **2019**, *17*, 1736–1739. [CrossRef] [PubMed]
14. Amatuni, A.; Shuster, A.; Adibekian, A.; Renata, H. Concise Chemoenzymatic Total Synthesis and Identification of Cellular Targets of Cepafungin, I. *Cell Chem. Biol.* **2020**, *27*, 1318–1326. [CrossRef] [PubMed]
15. Huang, Y.; Ji, X.; Ma, Z.; Łężyk, M.; Huang, Y.; Zhao, H. Green chemical and biological synthesis of cadaverine: Recent development and challenges. *RSC Adv.* **2021**, *11*, 23922–23942. [CrossRef]
16. Becker, J.; Wittmann, C. Diamines for bio-based materials. *Ind. Biotechnol. Prod. Process.* **2017**, 393–409. [CrossRef]
17. Kind, S.; Neubauer, S.; Becker, J.; Yamamoto, M.; Völkert, M.; von Abendroth, G.; Zelder, O.; Wittmann, C. From zero to hero—Production of bio-based nylon from renewable resources using engineered *Corynebacterium glutamicum*. *Metab. Eng.* **2014**, *25*, 113–123. [CrossRef]
18. Gómez, R.V.; Varela, O. Synthesis of regioisomeric, stereoregular AABB-type polyamides from chiral diamines and diacids derived from natural amino acids. *Tetrahedron Asymmetry* **2007**, *18*, 2190–2196. [CrossRef]
19. Kakwere, H.; Perrier, S. Design of complex polymeric architectures and nanostructured materials/hybrids by living radical polymerization of hydroxylated monomers. *Polym. Chem.* **2011**, *2*, 270–288. [CrossRef]
20. Orgueira, H.A.; Erra-Balsells, R.; Nonami, H.; Varela, O. Synthesis of chiral polyhydroxy polyamides having chains of defined regio and stereoregularity. *Macromolecules* **2001**, *34*, 687–695. [CrossRef]
21. Prell, C.; Vonderbank, S.-A.; Meyer, F.; Pérez-García, F.; Wendisch, V.F. Metabolic engineering of *Corynebacterium glutamicum* for de novo production of 3-hydroxycadaverine. *Curr. Res. Biotechnol.* **2021**, *4*, 32–46. [CrossRef]

22. Baud, D.; Peruch, O.; Saaidi, P.L.; Fossey, A.; Mariage, A.; Petit, J.L.; Salanoubat, M.; Vergne-Vaxelaire, C.; de Berardinis, V.; Zaparucha, A. Biocatalytic Approaches towards the Synthesis of Chiral Amino Alcohols from Lysine: Cascade Reactions Combining alpha-Keto Acid Oxygenase Hydroxylation with Pyridoxal Phosphate- Dependent Decarboxylation. *Adv. Synth. Catal.* **2017**, *359*, 1563–1569. [CrossRef]
23. Baud, D.; Saaidi, P.-L.L.; Monfleur, A.; Harari, M.; Cuccaro, J.; Fossey, A.A.; Besnard, M.; Debard, A.; Mariage, A.; Pellouin, V.; et al. Synthesis of Mono- and Dihydroxylated Amino Acids with New α-Ketoglutarate-Dependent Dioxygenases: Biocatalytic Oxidation of C–H Bonds. *ChemCatChem* **2014**, *6*, 3012–3017. [CrossRef]
24. Hara, R.; Yamagata, K.; Miyake, R.; Kawabata, H.; Uehara, H.; Kino, K.; Baud, D.; Saaidi, P.L.; Monfleur, A.; Harari, M.; et al. Discovery of Lysine Hydroxylases in the Clavaminic Acid Synthase-Like Superfamily for Efficient Hydroxylysine Bioproduction. *Appl. Environ. Microbiol.* **2017**, *83*, e00693-17. [CrossRef] [PubMed]
25. Bastard, K.; Isabet, T.; Stura, E.A.; Legrand, P.; Zaparucha, A. Structural Studies based on two Lysine Dioxygenases with Distinct Regioselectivity Brings Insights into Enzyme Specificity within the Clavaminate Synthase-Like Family. *Sci. Rep.* **2018**, *8*, 16587. [CrossRef] [PubMed]
26. Mcdonough, M.A.; Loenarz, C.; Chowdhury, R.; Clifton, I.J.; Schofield, C.J. Structural studies on human 2-oxoglutarate dependent oxygenases. *Curr. Opin. Struct. Biol.* **2010**, *20*, 659–672. [CrossRef]
27. Rolf, J.; Nerke, P.; Britner, A.; Krick, S.; Lütz, S.; Rosenthal, K. From cell-free protein synthesis to whole-cell biotransformation: Screening and identification of novel α-ketoglutarate-dependent dioxygenases for preparative-scale synthesis of hydroxy-L-lysine. *Catalysts* **2021**, *11*, 1038. [CrossRef]
28. Busch, F.; Busch, F.; Brummund, J.; Calderini, E.; Schürmann, M.; Kourist, R. Cofactor Generation Cascade for α-Ketoglutarate and Fe(II)-Dependent Dioxygenases. *ACS Sustain. Chem. Eng.* **2020**, *8*, 8604–8612. [CrossRef]
29. Mantri, M.; Zhang, Z.; McDonough, M.A.; Schofield, C.J. Autocatalysed oxidative modifications to 2-oxoglutarate dependent oxygenases. *FEBS J.* **2012**, *279*, 1563–1575. [CrossRef]
30. Fessner, W.D. Systems Biocatalysis: Development and engineering of cell-free "artificial metabolisms" for preparative multi-enzymatic synthesis. *New Biotechnol.* **2015**, *32*, 658–664. [CrossRef]
31. Tufvesson, P.; Lima-Ramos, J.; Nordblad, M.; Woodley, J.M. Guidelines and Cost Analysis for Catalyst Production in Biocatalytic Processes. *Org. Process Res. Dev.* **2011**, *15*, 266–274. [CrossRef]
32. Cassimjee, K.E.; Federsel, H.J. Chapter 13: EziG: A Universal Platform for Enzyme Immobilisation. *RSC Catal. Ser.* **2018**, *29*, 345–362. [CrossRef]
33. Encell, L.P. Development of a Dehalogenase-Based Protein Fusion Tag Capable of Rapid, Selective and Covalent Attachment to Customizable Ligands. *Curr. Chem. Genom.* **2013**, *6*, 55–71. [CrossRef] [PubMed]
34. Döbber, J.; Pohl, M. HaloTag^{TM}: Evaluation of a covalent one-step immobilization for biocatalysis. *J. Biotechnol.* **2017**, *241*, 170–174. [CrossRef] [PubMed]
35. Döbber, J.; Pohl, M.; Ley, S.V.; Musio, B. Rapid, selective and stable HaloTag-*Lb*ADH immobilization directly from crude cell extract for the continuous production of chiral alcohols and epoxides. *React. Chem. Eng.* **2018**, *3*, 8–12. [CrossRef]
36. Döbber, J.; Gerlach, T.; Offermann, H.; Rother, D.; Pohl, M. Closing the gap for efficient immobilization of biocatalysts in continuous processes: HaloTag^{TM} fusion enzymes for a continuous enzymatic cascade towards vicinal chiral diols. *Green Chem.* **2018**, *20*, 544–552. [CrossRef]
37. Sun, C.; Li, Y.; Taylor, S.E.; Mao, X.; Wilkinson, M.C.; Fernig, D.G. HaloTag is an effective expression and solubilisation fusion partner for a range of fibroblast growth factors. *PeerJ* **2015**, *2015*, 1–24. [CrossRef]
38. Rohman, M.; Harrison-Lavoie, K.J. Separation of copurifying GroEL from glutathione-S-transferase fusion proteins. *Protein Expr. Purif.* **2000**, *20*, 45–47. [CrossRef]
39. EnginZyme EziG TM Product Data Sheet. 2014, p. 9137. Available online: https://enginzyme.com/wp-content/uploads/2017/03/EziG%E2%84%A2-Product-Data-Sheet.pdf (accessed on 16 March 2022).
40. Grady, J.K.; Chasteen, N.D.; Harris, D.C. Radicals from "Good's" buffers. *Anal. Biochem.* **1988**, *173*, 111–115. [CrossRef]
41. Welch, K.D.; Davis, T.Z.; Aust, S.D. Iron autoxidation and free radical generation: Effects of buffers, ligands, and chelators. *Arch. Biochem. Biophys.* **2002**, *397*, 360–369. [CrossRef]
42. Tadolini, B. Iron autoxidation in mops and hepes buffers. *Free Radic. Res.* **1987**, *4*, 149–160. [CrossRef]
43. Ferreira, C.M.H.; Pinto, I.S.S.; Soares, E.V.; Soares, H.M.V.M. (Un)suitability of the use of pH buffers in biological, biochemical and environmental studies and their interaction with metal ions-a review. *RSC Adv.* **2015**, *5*, 30989–31003. [CrossRef]
44. Kivirikko, K.I.; Prockop, D.J. Partial purification and characterization of protocollagen lysine hydroxylase from chick embryos. *Biochem. Biophys. Acta Enzymol.* **1972**, *258*, 366–379. [CrossRef]
45. Liu, A.; Ho, R.Y.N.; Que, L.J. Alternative reactivity of an α-ketoglutarate-dependent iron(II) oxygenase: Enzyme self-hydroxylation. *J. Am. Chem. Soc.* **2001**, *123*, 5126–5127. [CrossRef] [PubMed]
46. Fossey-Jouenne, A.; Vergne-Vaxelaire, C.; Zaparucha, A. Enzymatic Cascade Reactions for the Synthesis of Chiral Amino Alcohols from L-lysine. *JoVE* **2018**, *132*, e56926. [CrossRef]
47. Sagong, H.; Son, H.F.; Kim, S.; Kim, Y.; Kim, K.; Kim, K. Crystal Structure and Pyridoxal 5-Phosphate Binding Property of Lysine Decarboxylase from *Selenomonas ruminantium*. *PLoS ONE* **2016**, *11*, e0166667. [CrossRef]
48. Jeong, S.; Yeon, Y.J.; Choi, E.; Byun, S.; Cho, D.; Kim, I.K.; Kim, Y.H. Alkaliphilic lysine decarboxylases for effective synthesis of cadaverine from L-lysine. *Korean J. Chem. Eng.* **2016**, *33*, 1530–1533. [CrossRef]

49. Takatsuka, Y.; Yamaguchi, Y.; Ono, M.; Kamio, Y. Gene Cloning and Molecular Characterization of Lysine Decarboxylase from *Selenomonas ruminantium* Delineate Its Evolutionary Relationship to Ornithine Decarboxylases from Eukaryotes. *J. Bacteriol.* **2000**, *182*, 6732–6741. [CrossRef] [PubMed]
50. Gerlach, T.; Nugroho, D.L.; Rother, D. The Effect of Visible Light on the Catalytic Activity of PLP-Dependent Enzymes. *ChemCatChem* **2021**, *13*, 2398–2406. [CrossRef]
51. Kind, S.; Jeong, W.K.; Schröder, H.; Zelder, O.; Wittmann, C. Identification and elimination of the competing N-acetyldiaminopentane pathway for improved production of diaminopentane by *Corynebacterium glutamicum*. *Appl. Environ. Microbiol.* **2010**, *76*, 5175–5180. [CrossRef]
52. Mi, J.; Liu, S.; Qi, H.; Huang, J.; Lan, X.; Zhang, L. Cellular Engineering and Biocatalysis Strategies toward Sustainable Cadaverine Production: State of the Art and Perspectives. *ACS Sustain. Chem. Eng.* **2021**, *9*, 1061–1072. [CrossRef]
53. Bhatia, S.K.; Kim, Y.H.; Kim, H.J.; Seo, H.M.; Kim, J.H.; Song, H.S.; Sathiyanarayanan, G.; Park, S.H.; Park, K.; Yang, Y.H. Biotransformation of lysine into cadaverine using barium alginate-immobilized *Escherichia coli* overexpressing CadA. *Bioprocess Biosyst. Eng.* **2015**, *38*, 2315–2322. [CrossRef]
54. Seo, H.M.; Kim, J.H.; Jeon, J.M.; Song, H.S.; Bhatia, S.K.; Sathiyanarayanan, G.; Park, K.; Kim, K.J.; Lee, S.H.; Kim, H.J.; et al. In situ immobilization of lysine decarboxylase on a biopolymer by fusion with phasin: Immobilization of CadA on intracellular PHA. *Process Biochem.* **2016**, *51*, 1413–1419. [CrossRef]
55. Zhou, N.; Zhang, A.; Wei, G.; Yang, S.; Xu, S.; Chen, K.; Ouyang, P. Cadaverine Production From L-Lysine with Chitin-Binding Protein-Mediated Lysine Decarboxylase Immobilization. *Front. Bioeng. Biotechnol.* **2020**, *8*, 103. [CrossRef] [PubMed]
56. Kloss, R.; Limberg, M.H.; Mackfeld, U.; Hahn, D.; Grünberger, A.; Jäger, V.D.; Krauss, U.; Oldiges, M.; Pohl, M. Catalytically active inclusion bodies of L-lysine decarboxylase from *E. coli* for 1,5-diaminopentane production. *Sci. Rep.* **2018**, *8*, 5856. [CrossRef] [PubMed]
57. Park, S.H.; Soetyono, F.; Kim, H.K. Cadaverine production by using cross-linked enzyme aggregate of *escherichia coli* lysine decarboxylase. *J. Microbiol. Biotechnol.* **2017**, *27*, 289–296. [CrossRef]
58. Lemonnier, M.; Lane, D. Expression of the second lysine decarboxylate gene of *Escherichia coli*. *Microbiology* **1998**, *144*, 751–760. [CrossRef]
59. Kim, H.J.; Kim, Y.H.; Shin, J.H.; Bhatia, S.K.; Sathiyanarayanan, G.; Seo, H.M.; Choi, K.Y.; Yang, Y.H.; Park, K. Optimization of direct lysine decarboxylase biotransformation for cadaverine production with whole-cell biocatalysts at high lysine concentration. *J. Microbiol. Biotechnol.* **2015**, *25*, 1108–1113. [CrossRef]
60. Sabo, D.L.; Boeker, E.A.; Byers, J.B.; Waron, H.; Fischer, E.H. Purification and Physical Properties of Inducible *Escherichia coli* Lysine Decarboxylase. *Biochemistry* **1974**, *13*, 662–670. [CrossRef]
61. Shin, J.; Joo, J.C.; Lee, E.; Hyun, S.M.; Kim, H.J.; Park, S.J.; Yang, Y.H.; Park, K. Characterization of a Whole-Cell Biotransformation Using a Constitutive Lysine Decarboxylase from *Escherichia coli* for the High-Level Production of Cadaverine from Industrial Grade l-Lysine. *Appl. Biochem. Biotechnol.* **2018**, *185*, 909–924. [CrossRef]
62. Paczia, N.; Nilgen, A.; Lehmann, T.; Gätgens, J.; Wiechert, W.; Noack, S. Extensive exometabolome analysis reveals extended overflow metabolism in various microorganisms. *Microb. Cell Fact.* **2012**, *11*, 1–14. [CrossRef]
63. Bradford, M.M. A Rapid and Sensitive Method for the Quantitation Microgram Quantities of Protein Utilizing the Principle of Protein-Dye Binding. *Anal. Biochem.* **1976**, 248–254. [CrossRef]
64. Chen, R.F.; Scott, C.; Trepman, E. Fluorescence properties of o-phthaldialdehyde derivatives of amino acids. *BBA Protein Struct.* **1979**, *576*, 440–455. [CrossRef]